

The synthesis, structure, and electrochemical properties of $\text{Fe}(\text{C}\equiv\text{CC}\equiv\text{N})(\text{dppe})\text{Cp}$ and related compounds¹

Mark E. Smith, Richard L. Cordiner, David Albesa-Jové, Dmitri S. Yufit, František Hartl, Judith A.K. Howard, and Paul J. Low

Abstract: The cyanoacetylide complex $\text{Fe}(\text{C}\equiv\text{CC}\equiv\text{N})(\text{dppe})\text{Cp}$ (**3**) is readily obtained from sequential reaction of $\text{Fe}(\text{C}\equiv\text{CSiMe}_3)(\text{dppe})\text{Cp}$ with methyl lithium and phenyl cyanate. Complex **3** is a good metalloligand, and coordination to the metal fragments $[\text{RhCl}(\text{CO})_2]$, $[\text{Ru}(\text{PPh}_3)_2\text{Cp}]^+$, and $[\text{Ru}(\text{dppe})\text{Cp}^*]^+$ affords the corresponding cyanoacetylide-bridged heterobimetallic complexes. In the case of the 36-electron complexes $[\text{Cp}(\text{dppe})\text{Fe}-\text{C}\equiv\text{CC}\equiv\text{N}-\text{ML}_n]^{n+}$, spectroscopic and structural data are consistent with a degree of charge transfer from the iron centre to the rhodium or ruthenium centre via the C_3N bridge, giving rise to a polarized ground state. Electrochemical and spectroelectrochemical methods reveal significant interactions between the metal centres in the oxidized (35 electron) derivatives, $[\text{Cp}(\text{dppe})\text{Fe}-\text{C}\equiv\text{CC}\equiv\text{N}-\text{ML}_n]^{(n+1)+}$.

Key words: cyanide, cyanoacetylide, crystal structure.

Résumé : Le complexe cyanoacétylure $\text{Fe}(\text{C}\equiv\text{CC}\equiv\text{N})(\text{dppe})\text{Cp}$ (**3**) est facilement préparé par la réaction séquentielle du $\text{Fe}(\text{C}\equiv\text{CSiMe}_3)(\text{dppe})\text{Cp}$ avec le méthyllithium et le cyanate de phényle. Le complexe **3** est un bon métalloligand et sa coordination aux fragments métalliques $[\text{RhCl}(\text{CO})_2]$, $[\text{Ru}(\text{PPh}_3)_2\text{Cp}]^+$ et $[\text{Ru}(\text{dppe})\text{Cp}^*]^+$ conduit à la formation des complexes hétérobimétalliques à point cyanoacétylure. Dans le cas des complexes à 36 électrons $[\text{Cp}(\text{dppe})\text{Fe}-\text{C}\equiv\text{CC}\equiv\text{N}-\text{ML}_n]^{n+}$, les données spectroscopiques et structurales sont en accord avec un certain degré de transfert de charge du centre ferrique à rhodium ou au centre ruthénium par le biais du pont C_3N , ce qui conduit à un état fondamental polarisé. Les méthodes électrochimiques et spectroélectrochimiques révèlent l'existence d'interactions importantes entre les centres métalliques des dérivés oxydés (à 35 électrons) de formule générale $[\text{Cp}(\text{dppe})\text{Fe}-\text{C}\equiv\text{CC}\equiv\text{N}-\text{ML}_n]^{(n+1)+}$.

Mots clés : cyanure, cyanoacétylure, structure cristalline.

[Traduit par la Rédaction]

Introduction

The chemistry of organometallic complexes featuring unsaturated ligands has been a source of interest for decades, owing to the unusual physical properties and chemical reactivity that arises from the mixing of metal d and ligand π orbitals. Acetylides and acetylenes are among the most structurally simple unsaturated ligands, offering cylindrical symmetry about the $\text{C}\equiv\text{C}$ moiety, and a polarizable π system. However, these structurally simple ligands are remarkably electronically diverse, being capable of formally donating one to six electrons to metal fragments and frameworks through various combinations of the filled ligand σ and π orbitals.

Our interests in complexes featuring $\text{C}\equiv\text{C}$ based ligands stem from the rich electrochemical response of bimetallic polyynediyl systems (1), the coordinative flexibility of (poly)yne ligands (2), and the chemical, physical, and spectroscopic properties of metal complexes featuring polycarbon ligands that depend heavily on the mixing of metal and carbon orbitals (3). In seeking to extend these studies, and at the same time to explore the relationships that exist between acetylide, $[\text{C}\equiv\text{CR}]^-$, and isoelectronic cyanide, $[\text{C}\equiv\text{N}]^-$, based unsaturated ligands, we were drawn to the cyanoacetylide ligand, $[\text{C}\equiv\text{CC}\equiv\text{N}]^-$.

We have recently developed convenient syntheses of several ruthenium complexes featuring the cyanoacetylide ligand, such as $[\text{Ru}(\text{C}\equiv\text{CC}\equiv\text{N})(\text{PPh}_3)_2\text{Cp}]$ (4). In the process

Received 13 June 2005. Published on the NRC Research Press Web site at <http://canjchem.nrc.ca> on 23 February 2006.

Dedicated to Arthur J. Carty, a respected mentor and valued friend, in recognition of his outstanding contributions to science.

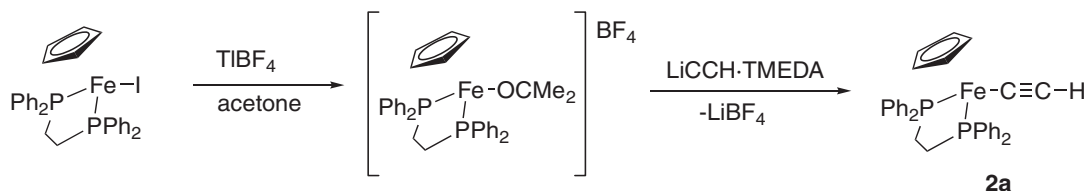
M.E. Smith, R.L. Cordiner, D. Albesa-Jové, D.S. Yufit, J.A.K. Howard, and P.J. Low.² Department of Chemistry, University of Durham, South Rd, Durham DH1 3LE, UK.

F. Hartl. Van't Hoff Institute for Molecular Sciences, University of Amsterdam, Nieuwe Achtergracht 166, 1018 WV Amsterdam, The Netherlands.

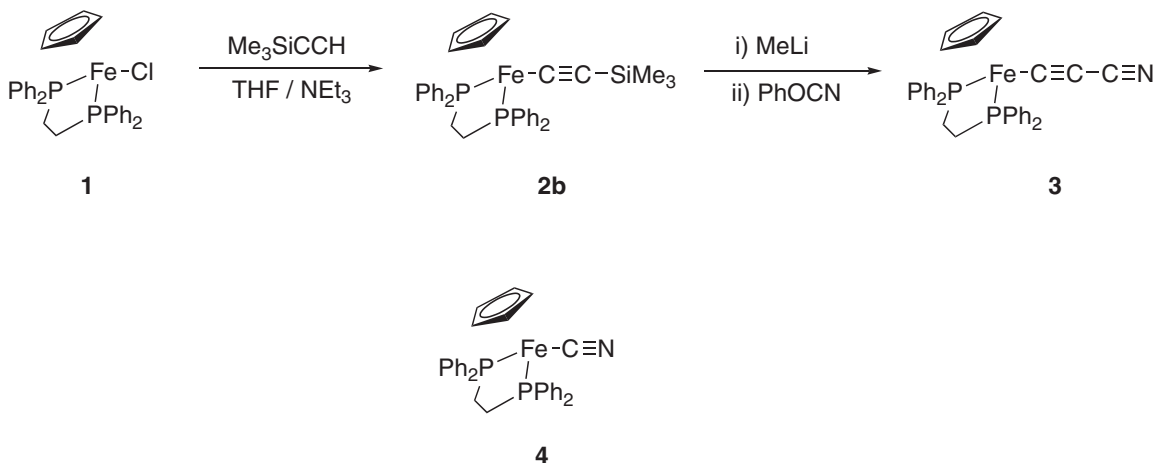
¹This article is part of a Special Issue dedicated to Professor Arthur Carty.

²Corresponding author (e-mail: p.j.low@durham.ac.uk).

Scheme 1.



Scheme 2.



of extending the synthetic methodology, we have had cause to prepare the related iron complex $[\text{Fe}(\text{C}\equiv\text{CC}\equiv\text{N})(\text{dppe})\text{Cp}]$ (**3**). In this paper we describe the synthesis, molecular structure, and electrochemical response of **3**, together with those of several related complexes.

Results and discussion

Acetylide complexes featuring the elementary structure $[\text{Fe}(\text{C}\equiv\text{CR})(\text{dppx})\text{Cp}]$ (dppx = bis(diphenylphosphino)methane, dppm; 1,2-bis(diphenylphosphino)ethane, dppe) are well-known (5), yet in recent times the development of the chemistry of this system has fallen behind that of the more electron-rich and sterically encumbered $[\text{Fe}(\text{C}\equiv\text{CR})(\text{dppe})\text{Cp}^*]$ analogues ($\text{Cp}^* = \eta^5\text{-C}_5\text{Me}_5$) (6). This is somewhat surprising given the quite straightforward synthesis of the key reagent $[\text{FeCl}(\text{dppe})\text{Cp}]$ (**1a**) (7).

In seeking to access an iron cyanoacetylide complex of the general form $[\text{Fe}(\text{C}\equiv\text{CC}\equiv\text{N})(\text{dppe})\text{Cp}]$, we required access to a synthon for the nucleophilic acetylide anion $[\text{Fe}(\text{C}\equiv\text{C}^-)(\text{dppe})\text{Cp}]$. Although $\text{Fe}(\text{C}\equiv\text{CH})(\text{dppe})\text{Cp}$ (**2a**) is a known compound (5b), the existing synthesis (reaction of $[\text{Fe}(\text{dppe})\text{Cp}]^+$ with $[\text{LiC}\equiv\text{CH}\cdot\text{TMEDA}]$) (Scheme 1) was not considered to be optimal given the many advances in synthetic transition metal acetylide chemistry that have been made since the original report of this compound.

We chose instead to examine the possibility of preparing either **2a** or $[\text{Fe}(\text{C}\equiv\text{CSiMe}_3)(\text{dppe})\text{Cp}]$ (**2b**) by formation of the analogous vinylidene, and deprotonation in situ (8). Thus, reaction of $[\text{FeCl}(\text{dppe})\text{Cp}]$ with excess (4 equiv.) $\text{HC}\equiv\text{CSiMe}_3$ in $\text{THF}-\text{NEt}_3$ (1:1 volumetric ratio) resulted in a gradual colour change in the solution from dark purple to orange. Workup gave the orange trimethylsilyl-protected acetylide complex **2b** in high (~80%) yield (Scheme 2).

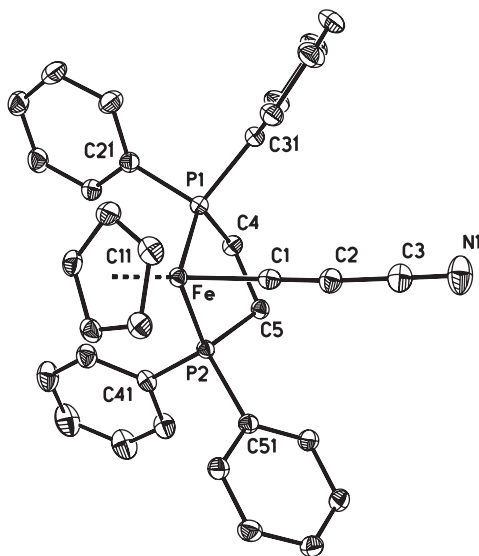
Further reaction of **2b** with MeLi (1.6 mol/L in diethyl ether) at low temperature gave an orange-yellow coloured solution containing the intermediate acetylide anion $[\text{Fe}(\text{C}\equiv\text{C}^-)(\text{dppe})\text{Cp}]$, which was not isolated but treated in situ with PhOCN to afford the cyanoacetylide complex $[\text{Fe}(\text{C}\equiv\text{CC}\equiv\text{N})(\text{dppe})\text{Cp}]$ (**3**) as a mustard-yellow coloured solid in 88% yield after chromatography and crystallization (Scheme 2). The cyanoacetylide complex was readily characterized from solution spectroscopic data, which included sharp singlets in the ^1H and ^{13}C NMR spectra arising from the Cp ligand (δ_{H} 4.29, δ_{C} 80.42), the phosphine resonance in the ^{31}P NMR spectrum (δ_{P} 104.91), and three carbon resonances arising from the cyanoacetylide ligand (δ_{C} 153.95, $J_{\text{CP}} = 37$ Hz (C_α); 106.13 (CN); 87.02 (C_β)). The C_α resonance, which was unambiguously assigned on the basis of the coupling to the dppe phosphorus nuclei, falls at the higher end of frequencies found in other acetylide complexes, $[\text{Fe}(\text{C}\equiv\text{CR})(\text{dppe})\text{Cp}^*]$ (6c). The cyanoacetylide ligand gave rise to two bands of moderate intensity at 2174 and 1991 cm^{-1} , which can be approximated as isolated $\nu(\text{CN})$ and $\nu(\text{CC})$ vibrations, but could also be a combination of vibrational modes.

The molecular structure of **3** (Fig. 1) was determined by single crystal X-ray diffraction (Table 1), and selected bond lengths and angles are summarized in Table 2. For purposes of comparison, the structure of the related cyanide complex $[\text{Fe}(\text{C}\equiv\text{N})(\text{dppe})\text{Cp}]$ (**4**) (9) was also determined (Fig. 2), while the complex $[\text{Fe}(\text{C}\equiv\text{CC}_6\text{H}_4\text{NO}_2)(\text{dppe})\text{Cp}]$ (**8**) provides a convenient set of metrical parameters associated with a metal acetylide featuring an electron-withdrawing group (10). The structures of **3**, **4**, and **8** show the expected gross similarities, with the iron centre adopting a pseudo-octahedral environment supported by the Cp ring, the chelating dppe ligand, and the C_nN ($n = 1$ (**4**), 3 (**3**)) or acetylide fragments.

Table 1. Crystallographic data for **3**, **4**, [6]PF₆, and [7]PF₆.

Compound code	3	4	[6]PF ₆	[7]PF ₆
Empirical formula	C ₃₅ H ₃₁ Cl ₂ FeNP ₂	C ₃₃ H ₃₁ Cl ₂ FeNP ₂	C _{75.50} H ₆₅ ClF ₆ FeN P ₅ Ru	C _{75.50} H ₆₅ ClF ₆ FeNP ₅ Ru
Formula weight	654.30	630.28	1 447.50	1 447.50
Temperature (K)	120(2)	120(2)	30(2)	120(2)
Crystal system	Triclinic	Monoclinic	Monoclinic	Monoclinic
Space group	<i>P</i> -1	<i>P</i> 2 ₁ / <i>n</i>	<i>P</i> 2 ₁ / <i>c</i>	<i>P</i> 2 ₁ / <i>c</i>
<i>a</i> (Å)	9.718(2)	12.8588(4)	14.6918(6)	14.6968(4)
<i>b</i> (Å)	12.415(3)	8.8080(3)	23.6085(9)	23.7690(7)
<i>c</i> (Å)	13.013(3)	25.7235(9)	19.5215(7)	19.6918(6)
α (°)	87.444(4)	90.00	90.00	90.00
β (°)	88.471(4)	90.862(2)	106.9440(10)	106.61(1)
γ (°)	76.206(4)	90.00	90.00	90.00
Volume (Å ³)	1 523.1(5)	2 913.12(17)	6 477.1(4)	6 591.9(3)
<i>Z</i>	2	4	4	4
<i>D</i> _c (Mg/m ³)	1.427	1.437	1.437	1.459
μ (mm ⁻¹)	0.802	0.835	0.649	0.673
Crystal size (mm)	0.25 × 0.24 × 0.16	0.26 × 0.24 × 0.22	0.40 × 0.32 × 0.16	0.20 × 0.18 × 0.18
θ Range (°)	2.81–30.51	1.58–30.52	1.45–30.45	1.68–28.00
Reflections collected	18 007	23 428	60 279	59 855
Independent reflections	9 055	8 857	19 302	15 905
<i>R</i> _(int)	0.0151	0.0427	0.1633	0.0446
<i>wR</i> (<i>F</i> ²) (<i>I</i> > 2 σ (<i>I</i>))	0.0829	0.1229	0.0856	0.1719
<i>R</i> (<i>F</i>) (<i>I</i> > 2 σ (<i>I</i>))	0.0317	0.0549	0.0755	0.0768
Refined parameters	458	352	882	807
GOF	1.068	1.154	1.227	1.192
$\Delta\rho_{\text{min,max}}$ (e Å ⁻³)	0.832 and -0.466	0.841 and -0.578	1.376 and -1.327	1.014 and -1.338

Fig. 1. The molecular structure of Fe(C≡CC≡N)(dppe)Cp (**3**), showing the atom labelling scheme. In this and all subsequent figures hydrogen atoms are omitted for clarity. Selected bond lengths (Å): Fe—C(1), 1.8526(13); C(1)—C(2), 1.2278(19); C(2)—C(3), 1.3672(19); C(3)—N(1), 1.1547(19); Fe—P(1), 2.1726(5); Fe—P(2), 2.1736(5); Fe—Cp(centroid), 1.711(1). Selected bond angles (°): Fe—C(1)—C(2), 176.03(11); C(1)—C(2)—C(3), 176.22(15); C(2)—C(3)—N(1), 178.97(17); P(1)—Fe—P(2), 86.27(2).



The Fe—Cp distances in **3** (2.086(1)–2.105(1) Å, avg. 2.09₅ Å) and **4** (2.093(2)–2.107(2) Å, avg. 2.10₁ Å) are longer than those in **8** (2.060(9)–2.088(10) Å, avg. 2.07₈ Å), as

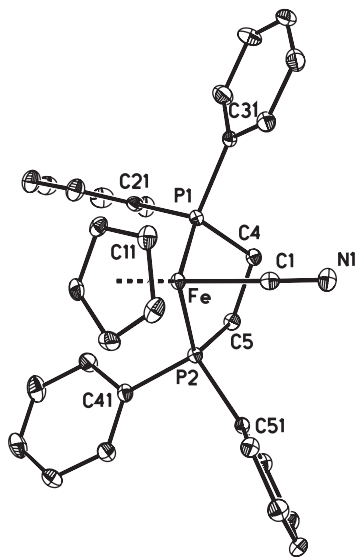
Table 2. Spectroelectrochemically generated IR data for compounds **3**, **3**⁺, [6]⁺, [6]²⁺, [7]⁺, and [7]²⁺.

Compound	$\nu(\text{C}\equiv\text{C}\equiv\text{N})$ (cm ⁻¹)
3	2174, 1991
3 ⁺	2201 (No other band observed)
[6] ⁺	2191, 1976
[6] ²⁺	2136, 1932
[7] ⁺	2189, 1984
[7] ²⁺	2121, 1946

are the the Fe—P (1, 2) bond lengths (**3**: 2.1736(5), 2.1726(5) Å; **4**: 2.1798(7), 2.1807(7) Å; **8**: 2.158(2), 2.157(2) Å). Interestingly, the intraring C—C distances in the cyclopentadienyl ring (**3**: avg. 1.42₁ Å; **4**: avg. 1.42₃ Å; **8**: avg. 1.37₆ Å) also display a degree of variation between the C_{*n*}N and acetylide complexes. Given the significance of back-bonding effects in M—Cp and M—P interactions, the structural trends in M—P and M—Cp bond lengths are consistent with either the decreased σ donation from the C_{*n*}N ligands relative to the acetylide ligand in **8**, and (or) a greater degree of iron-to-C_{*n*}N back-bonding. The Fe—C _{α} distance in all three complexes (**3**, **4**, and **8**) are similar (**3**: 1.853(1) Å; **4**: 1.893(2) Å; **8**: 1.856(8) Å), while the acetylide C≡C distance in **3** (1.228(2) Å) is indistinguishable from that in **8** (1.216(10) Å). Both observations argue against any statistically significant structural variation owing to a significant increase in back-bonding in **3** relative to **8**.

Numerous donor ligands (L) are known to react with the dimeric complex [RhCl(CO)₂]₂ resulting in cleavage of the chloride bridge, affording monomeric species *cis*-

Fig. 2. The molecular structure of $\text{Fe}(\text{C}\equiv\text{N})(\text{dppe})\text{Cp}$ (**4**), showing the atom labelling scheme. Selected bond lengths (Å): $\text{Fe}-\text{C}(1)$, 1.893(2); $\text{C}(1)-\text{N}(1)$, 1.167(3); $\text{Fe}-\text{P}(1)$, 2.1807(7); $\text{Fe}-\text{P}(2)$, 2.1798(7); $\text{Fe}-\text{Cp}(\text{centroid})$, 1.717(1). Selected bond angles (°): $\text{Fe}-\text{C}(1)-\text{N}(1)$, 178.6(2); $\text{P}(1)-\text{Fe}-\text{P}(2)$, 84.84(2).

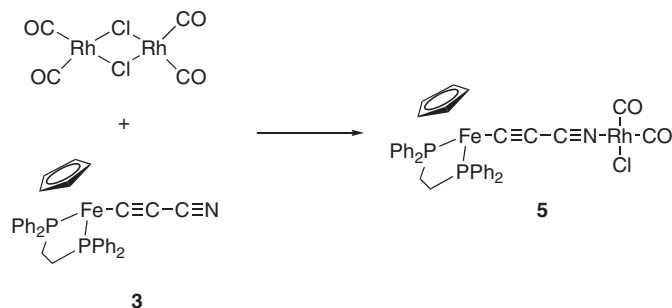


$[\text{RhCl}(\text{L})(\text{CO})_2]$ or *cis*- $[\text{RhCl}(\text{L}_2)(\text{CO})]$ (**11**). The reaction of **3** with $[\text{RhCl}(\text{CO})_2]_2$ proceeded smoothly in MeOH to afford *cis*- $[\text{RhCl}\{\text{N}\equiv\text{CC}\equiv\text{CFe}(\text{dppe})\text{Cp}\}(\text{CO})_2]$ (**5**) as a pale orange solid after purification of the reaction mixture by chromatography (Scheme 3).

The *cis* geometry about the rhodium centre was unequivocally established from the IR spectrum, which revealed $\nu(\text{CO})$ bands at 2085 and 2015 cm^{-1} in addition to the characteristic bands of the $\text{C}\equiv\text{C}\equiv\text{N}$ fragment at 2199 and 1978 cm^{-1} , and the ^{13}C NMR spectrum that contained a pair of doublets at 182.28 and 179.25 ppm arising from the two carbonyl ligands that are coupled to the Rh nucleus (Fig. 3). Similar data are associated with complexes derived from aminophosphines and point to the considerable donor character of the iron cyanoacetylide “metalloligand” (**11**). The ^{13}C NMR spectrum also revealed the remarkably high-frequency C_α resonance, which was observed as a triplet ($J_{\text{CP}} = 36$ Hz) at 177.23 ppm. Whilst the IR data clearly argue against a cumulenic description of the cyanocarbon ligand, the high-frequency ^{13}C shift of C_α supports the concept of a considerably polarized structure, with the electron-rich $\text{Fe}(\text{dppe})\text{Cp}$ fragment donating considerable electron density to the $\text{RhCl}(\text{CO})_2$ fragment via the $\text{C}\equiv\text{C}\equiv\text{N}$ bridge, which also carries a dipole moment in the same orientation.

We have recently described the synthesis of the 36-electron ruthenium and mixed iron–ruthenium diyndiyl complexes $[\{\text{Cp}'(\text{L}_2)\text{Ru}\}(\mu-\text{C}\equiv\text{CC}\equiv\text{C})\{\text{Ru}(\text{L}_2)\text{Cp}'\}]$ and $[\{\text{Cp}^*(\text{dppe})\text{Fe}\}(\mu-\text{C}\equiv\text{CC}\equiv\text{C})\{\text{Ru}(\text{L}_2)\text{Cp}'\}]$ ($\text{L} = \text{PPh}_3$, $\text{Cp}' = \text{Cp}$; $\text{L}_2 = \text{dppe}$, $\text{Cp}' = \text{Cp}^*$), together with the properties of the electrochemically accessible 35- and 34-electron oxidation products (**1b**, **1c**, **12**). The demonstration of considerable interaction between the heterometallic centres in **5** and predominant role of the ruthenium centre in determining the electronic properties of the mixed-metal diyndiyl system prompted us to consider the use of **3** in the preparation of

Scheme 3.



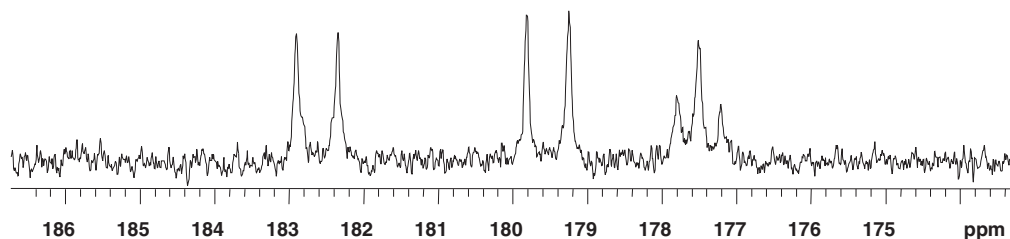
the cyanoacetylide-bridged complex, $[\{\text{Cp}(\text{dppe})\text{Fe}\}(\mu-\text{C}\equiv\text{CC}\equiv\text{N})\{\text{Ru}(\text{PPh}_3)_2\text{Cp}\}]\text{PF}_6$ (**[6]PF₆**).

Reaction of **3** with $\text{RuCl}(\text{PPh}_3)_2\text{Cp}$ in MeOH containing NH_4PF_6 afforded a red solution from which **[6]PF₆** was isolated as a bright yellow crystalline solid after extraction (CH_2Cl_2) and precipitation (hexane) (Scheme 4). Coordination of the $\text{Ru}(\text{PPh}_3)_2\text{Cp}$ fragment to the nitrogen centre in **3** was evident from comparison of the spectroscopic data with the properties of model complexes such as **3** and $[\text{Ru}(\text{NCPH})(\text{PPh}_3)_2\text{Cp}]\text{PF}_6$ (**13**, **14**). IR spectroscopy revealed a shift in the characteristic cyanoacetylide bands from 2174 and 1991 cm^{-1} in **3** to 2192 and 1977 cm^{-1} in **[6]PF₆**. The presence of the distinct Cp ligands associated with iron and ruthenium were clearly observed in the ^1H NMR spectra (**[6]PF₆**: $\delta_{\text{H}}(\text{Fe})$ 4.35; $\delta_{\text{H}}(\text{Ru})$ 4.21; **3**: $\delta_{\text{H}}(\text{Fe})$ 4.29; $\delta_{\text{H}}[\text{Ru}(\text{NCPH})(\text{PPh}_3)_2\text{Cp}]\text{PF}_6$ 4.55), while the dppe and PPh_3 ligands in **[6]PF₆** gave rise to two singlet resonances in the ^{31}P NMR spectrum at 103.91 (cf. **3**: δ_{P} 104.91) and 42.20 ppm (cf. $[\text{Ru}(\text{NCPH})(\text{PPh}_3)_2\text{Cp}]\text{PF}_6$: δ_{P} 42.89 ppm), respectively. The complex cation **[6]⁺** was observed in the ES(+)-MS at m/z 1260.

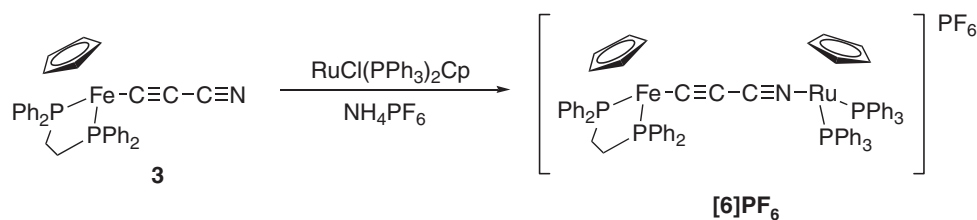
The complex $[\{\text{Cp}(\text{PPh}_3)_2\text{Ru}\}(\mu-\text{C}\equiv\text{CC}\equiv\text{N})\{\text{Fe}(\text{dppe})\text{Cp}\}]\text{PF}_6$ (**[7]PF₆**), a coordination (C/N bond) isomer of **[6]PF₆**, was prepared on a previous occasion from the reaction of $[\text{Ru}(\text{C}\equiv\text{CC}\equiv\text{N})(\text{PPh}_3)_2\text{Cp}]$ with **1a** (**4**) (Scheme 5). The spectroscopic properties of **[6]PF₆** and **[7]PF₆** are distinct, which rules out the possibility of ligand isomerism processes occurring during the syntheses. However, as complexes **[6]PF₆** and **[7]PF₆** are the first C/N bond isomers featuring the cyanoacetylide ligand, a concerted effort was made to crystallize both complexes, resulting in samples suitable for single crystal X-ray diffraction (Table 1).

The structures of the cations **[6]⁺** (Fig. 4) and **[7]⁺** (Fig. 5) illustrate a number of unusual features. The compounds are isostructural and in both of them the molecules of the metal complex are disordered over two positions (Fig. 4, Fig. 5). The disorder is rather unusual and the two possible orientations differ by interchange of the positions of the ethane bridge and FeCp moiety. Inevitably, three out of four atoms of the central C_3N link in both compounds are also disordered, while the atom coordinated to the Ru centre (N1 (**[6]⁺**); C1 (**[7]⁺**)) has large anisotropic displacement parameters. At the same time, the P(1) Ph_2 and P(2) Ph_2 fragments, which are coordinated to the iron centre, are identical in both conformations. The disorder is static, with the structure of **[6]PF₆** remaining disordered in the same fashion at temperatures between 120 and 30 K. The structures of **[6]PF₆**

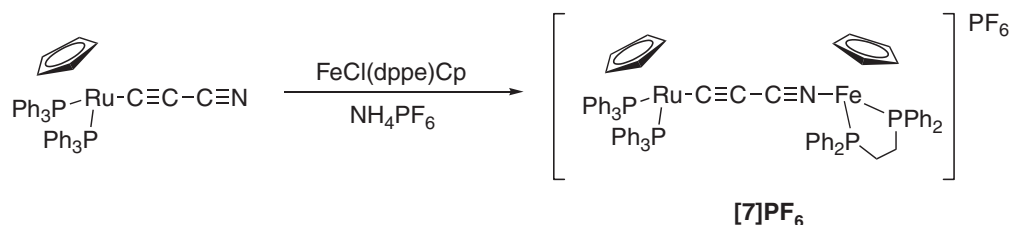
Fig. 3. The 175–185 ppm region of the ^{13}C NMR spectrum of **5** showing the distinct CO and C_α resonances.



Scheme 4.



Scheme 5.



and $[7]\text{PF}_6$ also contain disordered PF_6 anions and molecules of the crystallization solvent, CH_2Cl_2 .

Although variations in the relative disposition of the metal fragments about a diynidyl ($\text{C}\equiv\text{CC}\equiv\text{C}$) ligand are common (15), demonstrating the low energy of rotation of the metal fragment about the $\text{M}-\text{C}_\alpha$ bond, the observation of both cisoid and transoid forms within the same crystal lattice in the case of $[6]\text{PF}_6$ and $[7]\text{PF}_6$ is most unusual. It is also unusual that the same disorder results from the rotation of the $\text{Fe}(\text{dppe})\text{Cp}$ fragment about both $\text{Fe}-\text{C}$ ($[6]\text{PF}_6$) and $\text{Fe}-\text{N}$ ($[7]\text{PF}_6$) bonds.

In spite of the disorder, the distinct metal–C/N bond lengths in $[6]\text{PF}_6$ and $[7]\text{PF}_6$ reflect the different metal fragment coordinated at the C and N termini of the C_3N bridge, e.g., $\text{Ru}-\text{N}(1) = 2.054(4)$ Å in $[6]\text{PF}_6$ and $\text{Ru}-\text{C}(1) = 1.971(5)$ Å in $[7]\text{PF}_6$; $\text{Fe}-\text{C}(1) = 1.845(8)$ Å (transoid) and $1.86(1)$ (cisoid) Å in $[6]\text{PF}_6$, $\text{Fe}-\text{N}(1) = 1.904(6)$ Å (transoid) and $1.92(1)$ Å (cisoid) in $[7]\text{PF}_6$. The $\text{C}(2)\equiv\text{N}(1)$ bond length in each conformation of $[6]^+$ (1.183(9), 1.18(1) Å) is longer than the $\text{C}(3)\equiv\text{N}(4)$ bond length in the corresponding conformation of $[7]^+$ (1.16(2), 1.161(9) Å), but the other parameters are generally similar. Curiously, the $\text{Fe}-\text{P}$ bond lengths are significantly longer in the cisoid conformation of $[6]^+$ (2.138(2), 2.140(2) Å) than the transoid form (2.117(2), 2.116(2) Å). Back-bonding interactions will influence these $\text{Fe}-\text{P}$ bond lengths, and we speculate that these $\text{Fe}-\text{P}$ bond lengths indicate the different conformations observed in the solid state might arise from better transmission of electronic effects among the metal centres in the transoid geometry.

The combination of spectroscopic and structural data associated with the bimetallic complexes provides clear evidence for a degree of interaction between the metal centres through the polarized $\text{C}\equiv\text{CC}\equiv\text{N}$ bridging ligand. In an effort to further quantify these interactions, combined electrochemical and spectroelectrochemical (UV–vis–NIR, IR) investigations were carried out. Potentials reported here are referenced against internal ferrocene or decamethyl ferrocene standards as detailed in the Experimental section.

Complex **3** undergoes a single, reversible oxidation event at +0.53 V, which compares to that of the cyanide complex **4** at +0.55 V (16). Under the same conditions, the oxidation potential of $[\text{Ru}(\text{C}\equiv\text{CC}\equiv\text{N})(\text{PPh}_3)_2\text{Cp}]$ falls at +0.92 V (4). The bimetallic complexes $[6]\text{PF}_6$ and $[7]\text{PF}_6$ each undergo two oxidation processes, the reversibility of which improves at subambient temperatures. The oxidation potentials of both heterobimetallic complexes, $[6]\text{PF}_6$ (+0.66, +1.34 V) and $[7]\text{PF}_6$ (+0.62, +1.22 V), are similar and do not correlate with a simple model based upon metal-centred oxidation events, but rather indicate a significant donor–acceptor interaction between the iron and ruthenium centres in agreement with the structural data described above.

To access spectroscopic data from the mono- and di-oxidized forms of **3**, $[6]\text{PF}_6$, and $[7]\text{PF}_6$ we turned to spectroelectrochemical methods. Although the oxidation events associated with each complex were reversible on the CV timescale at room temperature, bulk electrolysis reactions in the spectroelectrochemical cells were carried out at ca. -30 °C to restrict complications arising because of decomposition of the electrogenerated oxidation products. Oxi-

Fig. 4. Plots of the cation $[6]^+$ illustrating (a) the atom labelling scheme and (b) the disordered nature of the iron end-cap. Selected bond lengths (transoid/cisoid) (Å): Fe—C(1), 1.849(7)/1.864(10); C(1)—C(2), 1.237(10)/1.217(14); C(2)—C(3), 1.374(10)/1.370(13); C(3)—N(1), 1.184(8)/1.183(10); Ru(1)—N(1), 2.056(4); Fe—P(1), 2.1265(17)/2.151(2); Fe—P(2), 2.1248(14)/2.1493(19); Ru—P(3), 2.3423(10); Ru—P(4), 2.3367(11). Selected bond angles (°): Fe—C(1)—C(2), 163.7(5)/179.2(9); C(2)—C(3)—N(1), 175.7(8)/170.8(11); C(3)—N(1)—Ru, 163.7(5)/159.9(6); P(1)—Fe—P(2), 88.95(6)/87.68(7); P(3)—Ru—P(4), 104.21(4).

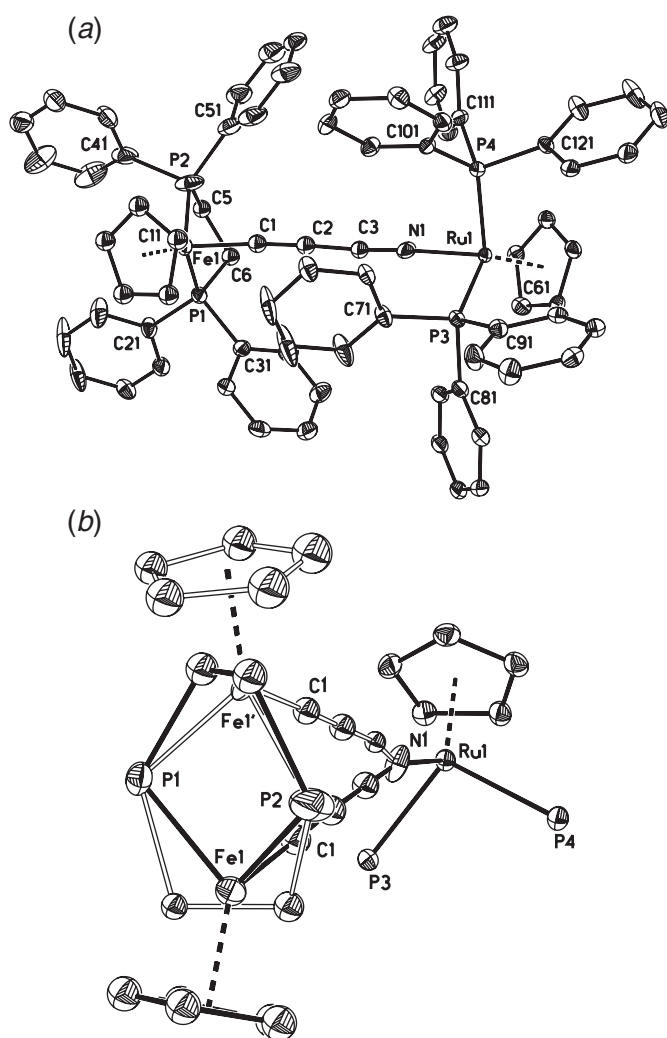
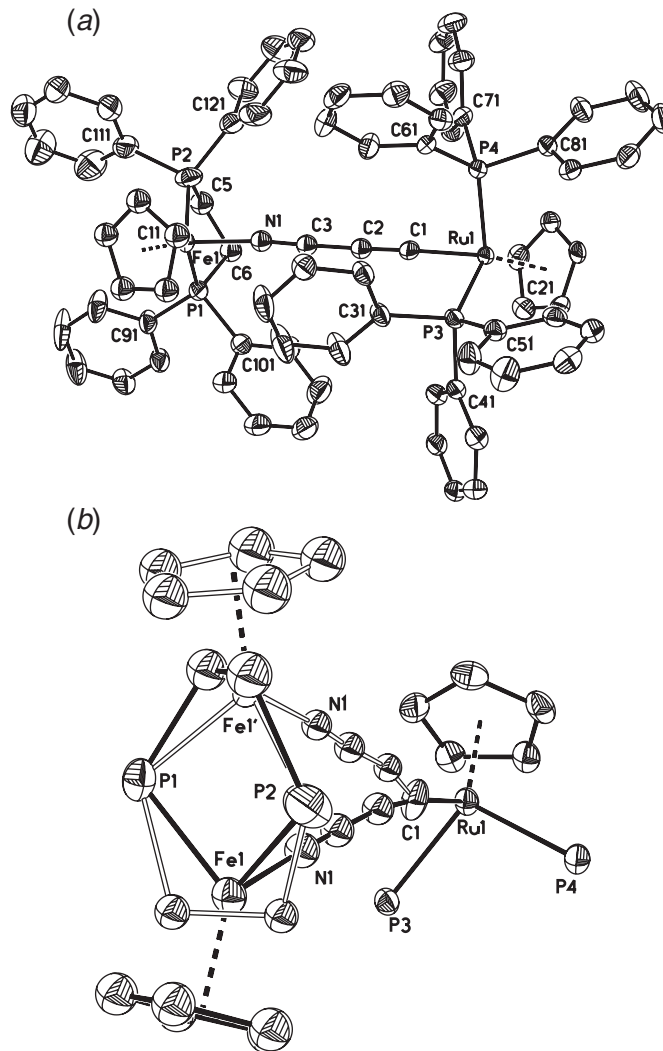


Fig. 5. An illustration of the disordered cation $[7]^+$ showing (a) the atom labelling scheme and (b) the disordered nature of the iron end-cap. Selected bond lengths (transoid/cisoid) (Å): Ru—C(1), 1.971(5); C(1)—C(2), 1.226(9)/1.318(16); C(2)—C(3), 1.374(10)/1.36(2); C(3)—N(1), 1.161(9)/1.16(3); Fe—N(1), 1.904(6)/1.916(13); Ru—P(3), 2.3093(13); Ru—P(4), 2.3090(13); Fe—P(1), 2.1310(18)/2.117(3); Fe—P(2), 2.147(2)/2.136(3). Selected bond angles (°): Ru—C(1)—C(2), 172.1(6)/157.1(8); C(1)—C(2)—C(3), 173.0(8)/168.6(16); C(2)—C(3)—N(1), 178.4(8)/176.7(17); C(3)—N(1)—Fe, 172.8(6)/175.9(13).



dation of $[\text{Fe}(\text{C}=\text{CC}=\text{N})(\text{dppe})\text{Cp}]$ (**3**) resulted in the collapse of the characteristic $\nu(\text{C}=\text{CC}=\text{N})$ bands of the unsaturated ligand and observation of a band at 2201 cm^{-1} of significantly lower intensity (Table 2). The pseudo $\nu(\text{C}=\text{C})$ band in this oxidized species, $[3]^+$, was not apparent, perhaps because of its low intensity. In contrast, two bands were observed following oxidation of the bimetallic complexes $[6]\text{PF}_6$ and $[7]\text{PF}_6$, which were shifted to lower energy by ca. $40\text{--}70\text{ cm}^{-1}$ in comparison with the spectra of the precursors, and therefore supporting the notion of an oxidation event that involves an orbital with an appreciable degree of ligand as well as metal character. In each case the original spectral profile was recovered after back-reduction of the oxidized samples.

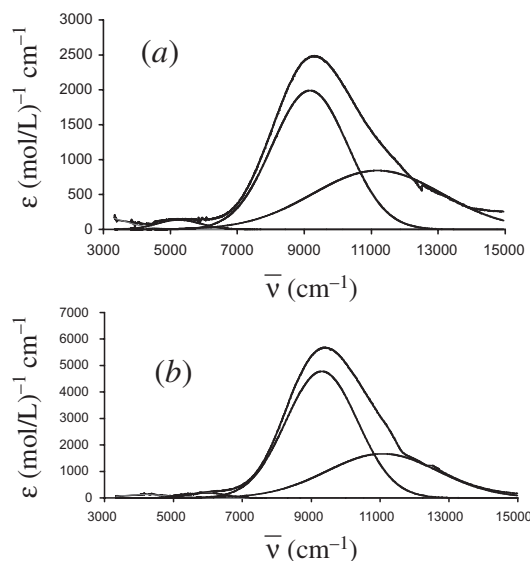
The electronic (UV–vis–NIR) spectrum of **3** changed little upon oxidation, and recovery of the original spectrum after back-reduction demonstrated the chemical reversibility of the electrochemical oxidation. Crucially, the NIR region of the spectrum remained transparent before and after oxidation of **3**. More interestingly, the one-electron oxidation products derived from $[6]\text{PF}_6$ and $[7]\text{PF}_6$ exhibited intense absorptions in the NIR region, each of which could be deconvoluted into three Gaussian-shaped absorption bands (Fig. 6, Table 3). Of these, the particularly low energy band of low intensity ($\bar{\nu}_{\text{max}}(\text{cm}^{-1})/\epsilon_{\text{max}} = 5260\text{ cm}^{-1}/140\text{ (mol/L)}^{-1}\text{ cm}^{-1}$ ($[6]^{2+}$); $5980\text{ cm}^{-1}/190\text{ (mol/L)}^{-1}\text{ cm}^{-1}$ ($[7]^{2+}$)) was approximated as a forbidden ligand–field transition associated with the oxidized iron centre ($6h$, $6k$, 17), which indicates that the

Table 3. Selected experimental and calculated band-shape parameters associated with the NIR bands exhibited by the 35-electron species, $[6]^{2+}$ and $[7]^{2+}$.

Band	$\bar{\nu}$ (cm ⁻¹), ϵ (mol/L) ⁻¹ cm ⁻¹	$\Delta\bar{\nu}_{1/2}$ (cm ⁻¹ , obs)	$\Delta\bar{\nu}_{1/2}$ (cm ⁻¹ , Hush)	H_{ab} (class II) ^a
$[6]^{2+}$ Band 1	9 175, 1 990	2650	4600	590
$[6]^{2+}$ Band 2	11 185, 840	4550	5080	555
$[7]^{2+}$ Band 1	9 310, 4 780	2445	4640	890
$[7]^{2+}$ Band 2	11 040, 1 665	3815	5050	710

^aCalculated using eq. [1] and assuming $d_{MM'} = 7.62 \text{ \AA}$, the average Fe—Ru separation obtained for both crystallographically determined cisoid and transoid conformations of $[6]PF_6$ and $[7]PF_6$.

Fig. 6. The deconvoluted NIR band envelopes associated with (a) $[6]^{2+}$ and (b) $[7]^{2+}$.



first oxidation event has some iron character in both C/N bond isomers.

Demandis et al. (18) have recently reviewed the properties of strongly coupled, ligand-bridged bimetallic mixed valence complexes, and described the various contributions of metal–ligand orbital mixing, spin-orbit coupling, and low symmetry, which lead to the three transitions that are in principle allowed between d^6 and d^5 metal ions to gather appreciable intensity. While the 35-electron, heterobimetallic dication $[6]^{2+}$ and $[7]^{2+}$ are not true mixed-valence species, similar considerations apply to the electronic spectra of these complexes. Since spin-orbit effects are relatively minor in lighter first and second row transition elements, the observation of multiple transitions in the NIR region of both species provides further evidence that the electronic structure of these heterometallic systems features a considerable degree of metal–ligand mixing. The band energy and shape are remarkably similar for both $[6]^{2+}$ and $[7]^{2+}$, and consequently similar transitions, and hence underlying electronic structures, are involved in both isomers.

The relationships originally derived by Hush (19) provide a vehicle for comparison of the electron-transfer processes occurring through the cyanoacetylide ligand in the complexes reported here with those observed in a large number of cyanide-bridged examples (20). Using the deconvoluted band shapes, and assuming that electron-transfer distance is

approximated by the crystallographically determined metal–metal separation, a coupling parameter (H_{ab}) may be calculated for each band using the expression give in eq. [1] (Table 3) (19).

$$[1] \quad H_{ab} = \frac{0.0205 \sqrt{\bar{\nu}_{\max} \epsilon \Delta \bar{\nu}_{1/2}}}{d'_{MM}}$$

Typically, values of H_{ab} for heterometallic cyanide bridged d^5/d^6 bimetallic complexes are in the range 1000–1700 cm⁻¹ when the NIR band shape data is treated in an entirely similar fashion. We note, however, that the use of the metal–metal distance is only a crude approximation of the electron-transfer distance, and given the involvement of the ligand orbitals in the SOMO, the real electron-transfer distance is likely to be considerably shorter. The values of H_{ab} reported in Table 3 represent a lower limit for the value of this parameter.

Whilst the availability of these 35-electron species as isolated samples would have greatly facilitated this study by allowing ready measurement of the solvent dependence of the NIR bands and permitted access to Mössbauer and magnetic data, it is unfortunate that at the present time we have been unable to chemically isolate samples of $[6]^{2+}$ or $[7]^{2+}$ as salts with common counterions. However, efforts in this area are ongoing, and with the possibility of exchanging the Cp for Cp* and related substituted cyclopentadienyl ligands, together with the large variety of phosphine ligands that may be introduced at either metal centre, we are hopeful that further information regarding the electronic structure of these unusual cyanoacetylide-bridged heterobimetallic complexes will become available in due course.

Conclusion

The readily prepared substrate FeCl(dppe)Cp is a convenient reagent for the preparation of both acetylide and cyanoacetylide iron complexes. The iron–cyanoacetylide complex, $[Fe(C\equiv CC\equiv N)(dppe)Cp]$, is a good metalloligand, readily coordinating to $RhCl(CO)_2$ or $Ru(PPh_3)_2Cp$ fragments to afford heterometallic complexes featuring the $\mu-\eta^1(C), \eta^1(N)-C\equiv CC\equiv N$ ligand. Spectroscopic data are consistent with a significant degree of polarization in the structures of the 36-electron species, and relatively large values of the coupling constant H_{ab} in the electrochemically generated 35-electron (d^5/d^6) dication, $[\{Cp(dppe)Fe\}(\mu-C\equiv CC\equiv N)-\{Ru(PPh_3)_2Cp\}]^{2+}$, and its C/N bond isomer, $[\{Cp(PPh_3)_2-Ru\}(\mu-C\equiv CC\equiv N)\{Fe(dppe)Cp\}]^{2+}$.

Experimental

All reactions were carried out using standard Schlenk techniques under dry high-purity nitrogen. Solvents were dried using an Innovative Technologies solvent purification system, and degassed prior to use. Preparative TLC was carried out on 20 cm × 20 cm glass plates coated with silica gel (Merck G₂₅₄, 0.5 mm thick). Reagents were purchased and used as received. Compounds **1a** (7), **4** (9), and **[7]PF₆** (4) were prepared according to the literature methods. Crystals of **4** and **[7]PF₆** suitable for X-ray diffraction were obtained from CH₂Cl₂–hexane and CH₂Cl₂–MeOH, respectively. IR spectra were recorded on a Nicolet Avatar FT IR spectrophotometer using solution cells fitted with CaF₂ windows. NMR spectra were obtained from solutions in CDCl₃ using Varian VXR-400 (¹H, 399.97 MHz; ¹³C, 100.57 MHz; ³¹P, 161.1 MHz) or Bruker DRX-400 (¹H, 400.13 MHz; ¹³C, 100.61 MHz; ³¹P, 162.05 MHz) spectrometers. Electrochemical experiments were conducted in CH₂Cl₂ solution containing 0.1 mol/L NBu₄PF₆ using a standard three-electrode cell (all Pt electrodes) and an EcoChemie Autolab PGSTAT-30. Potentials were corrected to SCE using an internal ferrocene/ferrocinium (Fc/Fc⁺ = 0.46 V) or decamethylferrocene/decamethylferrocinium couple as standard (Fc*/Fc*⁺ = 0.084 V).

IR spectroelectrochemical studies

IR spectroelectrochemical experiments at low temperatures were performed with a cryostated, optically transparent thin-layer electrochemical (OTTLE) cell equipped with CaF₂ windows and a Pt minigrad working electrode (32 wires/cm) (21). The electrolyses at room temperature were conducted with another homemade demountable OTTLE cell (22). The CH₂Cl₂ employed solutions were typically 3 × 10⁻¹ mol/L in the supporting electrolyte (NBu₄PF₆) and 10⁻³ mol/L in the analyte. The working electrode potential of the spectroelectrochemical cell was controlled with a PA4 potentiostat (EKOM, Polná, Czech Republic). The IR spectra were recorded with Bio-Rad FTS-7 and Bruker Vertex 70 FT IR spectrometers (16 scans, 1 to 2 cm⁻¹ spectral resolution).

UV–vis–NIR spectroelectrochemical studies

UV–vis–NIR were carried out using a Varian Cary 5 spectrophotometer in an OTTLE cell similar to that described previously (23) from solutions in CH₂Cl₂ containing 10⁻¹ mol/L NBu₄BF₄ as supporting electrolyte. Typically analyte concentrations were 10⁻¹ mmol/L.

[Fe(C≡CSiMe₃)(dppe)Cp] (**2b**)

A Schlenk flask was charged with [FeCl(dppe)Cp] (2.0 g, 3.60 mmol), NaBPh₄ (1.48 g, 4.32 mmol), THF (75 mL), and NEt₃ (75 mL), and the resulting dark solution treated with Me₃SiC≡CH (1.77 g, 2.54 mL, 18.0 mmol). After stirring for 16 h the solution colour had turned deep orange. The solvent was removed and the residue extracted with Et₂O and pentane added. The combined solvent was removed resulting in precipitation of a dark orange solid (1.75 g, 79%). IR (CH₂Cl₂, cm⁻¹): 1984 ν(C≡C). ¹H NMR (CDCl₃) δ: 0.06 (s, 9H, SiMe₃), 2.12 (m, 2H, dppe), 2.81 (m, 2H, dppe), 4.32 (s, 5H, Cp), 7.04–8.11 (m, 20H, Ph). ¹³C{H} NMR (CDCl₃) δ: 1.00 (s, SiMe₃), 27.96–28.32 (m,

CH₂ dppe), 79.52 (s, Cp), 103.85 (s, C_β), 127.87 (dt, J_{CP} = 58, 4 Hz, m-Ph), 129.13 (d, J_{CP} = 42 Hz, p-Ph), 133.14 (dt, J_{CP} = 248, 5 Hz, o-Ph), 138.00–142.64 (m, i-Ph), 151.39 (t, J_{CP} = 39 Hz, C_α). ³¹P{H} NMR (CDCl₃) δ: 107.71 (s, dppe). ES(+)-MS (*m/z*): 616.9 [M + H]⁺. Anal. calcd. for C₃₆H₃₈FeP₂Si (%): C 70.13, H 6.21; found: C 69.94, H 6.32.

[Fe(C≡CC≡N)(dppe)Cp] (**3**)

A Schlenk flask was charged with [Fe(C≡CSiMe₃)(dppe)Cp] (500 mg, 0.81 mmol) in THF (20 mL). The orange/yellow solution was cooled to -78 °C and MeLi (0.6 mL, 0.96 mmol of a 1.6 mol/L solution in Et₂O) was added at such a rate as to prevent the temperature exceeding -50 °C. After stirring for 1 h the solution was warmed to -20 °C before being cooled again. To the orange/yellow solution was added PhOCN (0.5 mL, 0.9 mmol) and the solution allowed to come slowly to room temperature before the solvent was removed. The dark red/brown residue was dissolved in CH₂Cl₂ and purified by column chromatography on silica, the product eluting with acetone–hexane (30:70). Concentration of the dark red fraction resulted in the formation of a mustard yellow precipitate, which was collected, washed with hexane, and air dried to afford **3**, which was recrystallized from CH₂Cl₂–Et₂O (yield: 400 mg, 88%). IR (CH₂Cl₂, cm⁻¹): 2174, 1991 ν(C≡CC≡N). ¹H NMR (CDCl₃) δ: 2.32 (m, 2H, dppe), 2.60 (m, 2H, dppe), 4.29 (s, 5H, Cp), 7.74–6.85 (m, 20H, Ph). ¹³C{H} NMR (CDCl₃) δ: 27.88–28.35 (m, CH₂ dppe), 80.42 (s, Cp), 87.02 (s, C_β), 106.13 (s, CN), 127.99 (dt, J_{CP} = 26, 4 Hz, m-Ph), 129.58 (d, J_{CP} = 53 Hz, p-Ph), 132.23 (dt, J_{CP} = 167, 4 Hz, o-Ph), 135.55–140.21 (m, i-Ph), 153.95 (t, J_{CP} = 37 Hz, C_α). ³¹P{H} NMR (CDCl₃) δ: 104.91 (s, dppe). ES(+)-MS (*m/z*): 570.1 [M + H]⁺. Anal. calcd. for C₃₄H₂₉FeNP₂ (%): C 71.72, H 5.13, N 2.46; found: C 71.67, H 5.07, N 1.72.

[[Cp(dppe)Fe](μ-C≡CC≡N){cis-RhCl(CO)₂}] (**5**)

A Schlenk flask was charged with [Fe(C≡CC≡N)(dppe)Cp] (73 mg, 0.129 mmol), [RhCl(CO)₂]₂ (25 mg, 0.065 mmol), NH₄PF₆ (35 mg, 0.215 mmol), and MeOH (25 mL), and the resulting solution stirred for 48 h. The solvent was then removed and the residue extracted with CH₂Cl₂ and filtered through a small pad of silica. Addition of hexane to the CH₂Cl₂ solution and concentration resulted in an orange precipitate, which was collected, washed with pentane, and air dried (yield: 50 mg, 51%). IR (CH₂Cl₂, cm⁻¹): 2199, 1991 ν(C≡CC≡N); 2085, 2015 ν(CO). ¹H NMR (CDCl₃) δ: 2.37 (m, 2H, dppe), 2.60 (m, 2H, dppe), 4.36 (s, 5H, Cp), 7.68–7.17 (m, 20H, Ph). ¹³C{H} NMR (CDCl₃) δ: 28.24–28.59 (m, CH₂ dppe), 81.58 (s, Cp), 85.32 (s, C_β), 106.27 (s, CN), 128.30–139.41 (m, Ph), 177.23 (t, J_{CP} = 36 Hz, C_α), 179.25 (d, J_{RhC} = 70 Hz, CO cis to NC), 182.28 (d, J_{RhC} = 70 Hz, CO trans to NC). ³¹P{H} NMR (CDCl₃) δ: 103.45 (s, dppe). Anal. calcd. for C₃₆H₂₉ClFeNO₂P₂Rh (%): C 56.61, H 3.83, N 1.83; found: C 56.22, H 3.96, N 1.37.

[[Fe(dppe)Cp](C≡CC≡N){Ru(PPh₃)₂Cp}]PF₆ (**[6]PF₆**)

A Schlenk flask was charged with [Fe(C≡CC≡N)(dppe)Cp] (75 mg, 0.132 mmol), [RuCl(PPh₃)₂Cp] (96 mg, 0.132 mmol), and NH₄PF₆ (86 mg, 0.528 mmol). The mixture was suspended in MeOH (15 mL) and refluxed for 1 h after which time a dark red solution had formed. This was

allowed to cool and the solvent removed. The red/brown residue was extracted with CH_2Cl_2 and filtered into hexane. The resulting yellow precipitate was collected, washed with hexane, and air dried to afford $[\mathbf{6}]\text{PF}_6$ (yield: 105 mg, 57%). Crystals suitable for X-ray diffraction were obtained from CH_2Cl_2 -hexane. IR (CH_2Cl_2 , cm^{-1}): 2192, 1977 $\nu(\text{C}\equiv\text{CC}\equiv\text{N})$. ^1H NMR (CDCl_3) δ : 1.62 (br, 8H, dppe), 4.21, 4.35 ($2 \times$ s, 10H, $2 \times$ Cp), 6.97–7.64 (m, 40H, Ph). $^{31}\text{P}\{\text{H}\}$ NMR (CDCl_3) δ : -143.11 (ht, $J_{\text{PF}} = 711$ Hz, PF_6^-), 42.20 (s, PPh_3), 103.91 (s, dppe). ES(+)-MS (m/z): 1260 [$\{\text{Fe}(\text{dppe})\text{-Cp}\}\{\text{C}\equiv\text{CC}\equiv\text{N}\}\{\text{Ru}(\text{PPh}_3)_2\text{Cp}\}]^+$; 691 [$\text{Ru}(\text{PPh}_3)_2\text{Cp}\}]^+$. Despite repeated efforts to remove solvent from the analytical sample, this compound consistently analysed with 1/2 molecule of the CH_2Cl_2 crystallization solvent. Anal. calcd. for $\text{C}_{75}\text{H}_{64}\text{F}_6\text{FeNP}_5\text{Ru}\cdot 0.5\text{CH}_2\text{Cl}_2$ (%): C 62.64, H 4.53, N 0.97; found: C 62.29, H 4.43, N 0.91.

Crystallography

The X-ray data sets for compounds **3**, **4**, $[\mathbf{6}]\text{PF}_6$, and $[\mathbf{7}]\text{PF}_6$ were collected on Bruker 3-circle diffractometers with Bruker ProteumM diffractometer and Bede Microsource[®] (for **3**, **4**, and $[\mathbf{6}]\text{PF}_6$) or SMART 6K (for $[\mathbf{7}]\text{PF}_6$) CCD area detectors using graphite-monochromated sealed-tube Mo K_α radiation. The data collection was carried out at 120 K using cryostream (Oxford cryosystem) open flow N_2 cryostats. Reflection intensities were integrated using the SAINT program, version 6.02a (for **3** and $[\mathbf{6}]\text{PF}_6$) and version 6.45 (for **4** and $[\mathbf{7}]\text{PF}_6$) (24). The crystal structures were solved using direct-methods and refined by full matrix least-squares against F^2 of all data using SHELXTL software (25). All non-hydrogen atoms were refined in anisotropic approximation (for **3** and **4**). In the case of $[\mathbf{6}]\text{PF}_6$ and $[\mathbf{7}]\text{PF}_6$, the non-hydrogen atoms located in two different sites, PF_6^- anions, and solvent molecules were refined in isotropic approximation.

Hydrogen atoms were placed in calculated positions and refined using a riding model (for **4**, $[\mathbf{6}]\text{PF}_6$, and $[\mathbf{7}]\text{PF}_6$) or located by different Fourier maps and refined unconstrained (for **3**). All four crystal structures present dichloromethane molecules, and for $[\mathbf{6}]\text{PF}_6$ and $[\mathbf{7}]\text{PF}_6$ the solvent molecules are highly disordered with connectivity between atoms only visible for one dichloromethane molecule.

Crystal data and experimental details are listed in Table 1.³

Acknowledgements

We thank Taasje Mahabiersing (University of Amsterdam) for assistance with the electrochemical and spectroelectrochemical work. Financial assistance from the Engineering and Physical Sciences Research Council (EPSRC), OneNorthEast, and the EU ESSD HPMT-CT-2001-0311 Marie Curie Training Site (Amsterdam, The Netherlands) is gratefully acknowledged. RLC held a scholarship from the

University of Durham Chemistry EPSRC Doctoral Training Account.

References

- (a) M.I. Bruce and P.J. Low. *Adv. Organomet. Chem.* **50**, 179 (2004); (b) M.I. Bruce, P.J. Low, K. Costuas, J.F. Halet, S.P. Best, and G.A. Heath. *J. Am. Chem. Soc.* **122**, 1949 (2000); (c) M.I. Bruce, B.G. Ellis, P.J. Low, B.W. Skelton, and A.H. White. *Organometallics*, **22**, 3184 (2003).
- (a) P.J. Low and M.I. Bruce. *Adv. Organomet. Chem.* **48**, 71 (2002); (b) P.J. Low, K.A. Udachin, G.D. Enright, and A.J. Carty. *J. Organomet. Chem.* **578**, 103 (1999); (c) P.J. Low, T.M. Hayes, K.A. Udachin, A.E. Goeta, J.A.K. Howard, G.D. Enright, and A.J. Carty. *J. Chem. Soc. Dalton Trans.* 1455 (2002); (d) P.J. Low, K.A. Udachin, and A.J. Carty. *J. Cluster Sci.* **15**, 277 (2004); (e) O.F. Koentjoro, P.J. Low, R. Rousseau, C. Nervi, D.S. Yufit, J.A.K. Howard, and K.A. Udachin. *Organometallics*, **24**, 1284 (2005).
- (a) O.F. Koentjoro, R. Rousseau, and P.J. Low. *Organometallics*, **20**, 4502 (2001); (b) P.J. Low, R. Rousseau, P. Lam, K.A. Udachin, G.D. Enright, J.S. Tse, D.D.M. Wayner, and A.J. Carty. *Organometallics*, **18**, 3885 (1999); (c) P.J. Low, A.J. Carty, K.A. Udachin, and G.D. Enright. *Chem. Commun. (Cambridge)*, 411 (2001); (d) M.I. Bruce, K. Costuas, J.F. Halet, B.C. Hall, P.J. Low, B.K. Nicholson, B.W. Skelton, and A.H. White. *J. Chem. Soc. Dalton Trans.* 383 (2002); (e) R.L. Roberts, H. Puschmann, J.A.K. Howard, J.H. Yamamoto, A.J. Carty, and P.J. Low. *Dalton Trans.* 1099 (2003).
- R.L. Cordiner, D. Corcoran, D.S. Yufit, A.E. Goeta, J.A.K. Howard, and P.J. Low. *Dalton Trans.* 3541 (2003).
- (a) R. Nast. *Coord. Chem. Rev.* **47**, 89 (1982); (b) A. Davison and J.P. Selegue. *J. Am. Chem. Soc.* **100**, 7763 (1978); (c) S. Abbott, S.G. Davies, and P. Warner. *J. Organomet. Chem.* **246**, C65 (1983); (d) C.E. Powell, M.P. Cifuentes, A.M. McDonagh, S.K. Hurst, N.T. Lucas, C.D. Delfs, R. Stranger, M.G. Humphrey, S. Houbrechts, I. Asselberghs, A. Persoons, and D.C.R. Hockless. *Inorg. Chim. Acta*, **352**, 9 (2003); (e) N.G. Connelly, M.P. Gamasa, J. Gimeno, C. Lapinte, E. Lastra, J.P. Maher, N. Le Narvor, A.L. Rieger, and P.H. Rieger. *J. Chem. Soc. Dalton Trans.* 2575 (1993); (f) M.P. Gamasa, J. Gimeno, E. Lastra, M. Lanfranchi, and A. Tiripicchio. *J. Organomet. Chem.* **405**, 333 (1991).
- (a) X.H.S. Gu and M.B. Sponsler. *Organometallics*, **17**, 5920 (1998); (b) L. Dahlenburg, A. Weiss, M. Bock, and A. Zahl. *J. Organomet. Chem.* **541**, 465 (1997); (c) R. Denis, T. Weyland, F. Paul, and C. Lapinte. *J. Organomet. Chem.* **546**, 615 (1997); (d) S. Le Stang, D. Lenz, F. Paul, and C. Lapinte. *J. Organomet. Chem.* **572**, 189 (1999); (e) N. Le Narvor and C. Lapinte. *Organometallics*, **14**, 634 (1995); (f) F. Paul and C. Lapinte. *Coord. Chem. Rev.* **178**, 431 (1998); (g) S. Le Stang, F. Paul, and C. Lapinte. *Organometallics*, **19**, 1035 (2000); (h) T. Weyland, K. Costuas, L. Toupet, J.-F. Halet, and C. Lapinte. *Organometallics*, **19**, 4228 (2000); (i) F. Paul, W.E. Meyer, L. Toupet, H. Jiao, J.A. Gladysz, and C. Lapinte. *J. Am. Chem. Soc.* **122**, 9405 (2000); (j) T. Weyland, I. Ledoux, S. Brasselet, J. Zyss, and C. Lapinte. *Organometallics*, **19**, 5235

³Supplementary data for this article are available on the journal Web site (<http://canjchem.nrc.ca>) or may be purchased from the Depository of Unpublished Data, Document Delivery, CISTI, National Research Council Canada, Ottawa, ON K1A 0R6, Canada. DUD 4087. For more information on obtaining material refer to http://cisti-icist.nrc-cnrc.gc.ca/irm/unpub_e.shtml. CCDC 274245–274248 contain the crystallographic data for this manuscript. These data can be obtained, free of charge, via <http://www.ccdc.cam.ac.uk/contents/retrieving.html> (Or from the Cambridge Crystallographic Data Centre, 12 Union Road, Cambridge CB2 1EZ, UK; fax +44 1223 336033; or deposit@ccdc.cam.ac.uk).

- (2000); (k) S. Roué, C. Lapinte, and T. Bataille. *Organometallics*, **23**, 2558 (2004); (l) F. Coat, F. Paul, C. Lapinte, L. Toupet, K. Costuas, and J.-F. Halet. *J. Organomet. Chem.* **683**, 368 (2003); (m) M. Guillemot, L. Toupet, and C. Lapinte. *Organometallics*, **17**, 1928 (1998); (n) S. Roué and C. Lapinte. *J. Organomet. Chem.* **690**, 594 (2005).
7. M.J. Mays and P.L. Sears. *J. Chem. Soc. Dalton Trans.* 1873 (1973).
 8. (a) N. Le Narvor, L. Toupet, and C. Lapinte. *J. Am. Chem. Soc.* **117**, 7129 (1995); (b) F. Coat, P. Thominot, and C. Lapinte. *J. Organomet. Chem.* **629**, 39 (2001).
 9. G.J. Baird and S.G. Davies. *J. Organomet. Chem.* **262**, 215 (1984).
 10. M.H. Garcia, M.P. Robalo, A.R. Dias, M.T. Duarte, W. Wenseleers, A. Aerts, E. Goovaerts, M.P. Cifuentes, S. Hurst, M.G. Humphrey, M. Samoc, and B. Luther-Davies. *Organometallics*, **21**, 2107 (2002).
 11. P.W. Dyer, J. Fawcett, M.J. Hanton, R.D.W. Kemmitt, R. Padda, and N. Singh. *Dalton Trans.* 104 (2003).
 12. M.I. Bruce, K. Costuas, T. Davin, B.G. Ellis, J.F. Halet, C. Lapinte, P.J. Low, M.E. Smith, B.W. Skelton, L. Toupet, and A.H. White. *Organometallics*, **24**, 3864 (2005).
 13. G.S. Ashby, M.I. Bruce, I.B. Tomkins, and R.C. Wallis. *Aust. J. Chem.* **32**, 1003 (1979).
 14. R.L. Cordiner, D. Albesa-Jové, R.L. Roberts, J.D. Farmer, H. Puschmann, D. Corcoran, A.E. Goeta, J.A.K. Howard, and P.J. Low. *J. Organomet. Chem.* **690**, 4908 (2005).
 15. M.I. Bruce, B.G. Ellis, M. Gaudio, C. Lapinte, G. Melino, F. Paul, B.W. Skelton, M.E. Smith, L. Toupet, and A.H. White. *Dalton Trans.* 1601 (2004).
 16. G.N. Richardson, U. Brand, and H. Vahrenkamp. *Inorg. Chem.* **38**, 3070 (1999).
 17. S. Le Stang, F. Paul, and C. Lapinte. *Inorg. Chim. Acta*, **291**, 403 (1999).
 18. K.D. Demandis, C.M. Hartshorn, and T.J. Meyer. *Chem. Rev.* **101**, 2655 (2001).
 19. (a) C. Creutz, M.D. Newton, and N. Sutin. *J. Photochem. Photobiol. A: Chem.* **82**, 47 (1994); (b) J.-P. Launay. *Chem. Soc. Rev.* **30**, 386 (2001).
 20. C. Díaz and A. Arancibia. *Inorg. Chim. Acta*, **269**, 246 (1998).
 21. (a) F. Hartl, H. Luyten, H.A. Nieuwenhuis, and G.C. Schoemaker. *Appl. Spectrosc.* **48** 1522 (1994); (b) T. Mahabiersing, H. Luyten, R.C. Nieuwendam, and F. Hartl. *Coll. Czech. Chem. Commun.* **68** 1687 (2003).
 22. M. Krejčík, M. Danek, and F. Hartl. *J. Electroanal. Chem.* **317** 179 (1991).
 23. C.M. Duff and G.A. Heath. *Inorg. Chem.* **30**, 2528 (1991).
 24. (a) SAINT. Version 6.02a [computer program]. Bruker AXS, Madison, Wisconsin. 2001; (b) SAINT. Version 6.45 [computer program]. Bruker AXS, Madison, Wisconsin. 1998.
 25. SHELXTL. Version 5.10 [computer program]. Bruker AXS, Madison, Wisconsin. 1997.